

Effect of impurities on the electronic phase transition in graphite in the magnetic quantum limit

Y. Iye

AT&T Bell Laboratories, Murray Hill, New Jersey 07974

L. E. McNeil

Center for Materials Science and Engineering, Massachusetts Institute of Technology, Cambridge, Massachusetts 02139

G. Dresselhaus

Francis Bitter National Magnet Laboratory, Massachusetts Institute of Technology, Cambridge, Massachusetts 02139

(Received 16 April 1984; revised manuscript received 23 August 1984)

The electronic phase transition in graphite under strong magnetic fields is studied by magnetotransport measurement for a wide variety of single-crystal samples for a field range up to 280 kG and temperatures down to 0.41 K. The magnetic field dependence of the transition temperature is fitted to a functional form, $T_c(B) = T^* \exp(-B^*/B)$, where the parameters T^* and B^* are approximately 100 K and 1000 kG, respectively. This functional form is consistent with Yoshioka and Fukuyama's model of a magnetic-field-induced charge-density-wave instability. We have found two types of samples, each of which exhibit distinctive magnetotransport behavior at the onset of the phase transition. For one sample type, we have observed a suppression of T_c and a less sharp conductivity change at the transition point, relative to the other type. This difference in behavior is correlated with the difference in the ionized impurity concentration between the two types of samples as deduced from the high-field Hall measurements. The differences between the types can be understood by taking account of the "pair-breaking" effect of the impurities.

I. INTRODUCTION

The possibility of a magnetic-field-induced phase transition of an electron gas into a Wigner crystal or a charge-density-wave (CDW) state has been discussed theoretically by several authors.¹⁻⁵ On the experimental side, such a Wigner or CDW transition has been invoked by several authors as a possible explanation of anomalies observed in magnetotransport and other kinds of experiments.⁶⁻⁹

Among three-dimensional systems, the possibility has been pursued in degenerate semiconductors such as InSb (Ref. 6) and $\text{Hg}_{1-x}\text{Cd}_x\text{Te}$ (Ref. 7) by means of transport measurements. However, the experimental situation is not very clear in these materials. Namely, since the carriers in these systems at low temperatures are extrinsic in nature, there always is a possibility of the so-called magnetic freezeout effect, which would yield transport anomalies apparently similar to those expected for the CDW phase transition. In view of this, a system with intrinsic carriers provides a clearer model for the possible CDW transition. Among the degenerate systems, a low carrier concentration is favored both for the dominance of the Coulomb energy over the kinetic energy and for accessibility to the extreme-quantum-limit condition. Hence, semimetals such as Bi, Bi-Sb alloys, and graphite provide good candidates for the study of magnetic-field-induced CDW phase transition.

Recently, we have discovered an anomaly in the high-field magnetoresistance of graphite.¹⁰⁻¹² The abruptness of the resistivity change and the strong temperature dependence of the onset field have suggested an oc-

currence of an electronic phase transition. Stimulated by the experiment, Yoshioka and Fukuyama¹³ have proposed a theoretical model for the phenomenon based on Fukuyama's theory of the magnetic-field-induced CDW transition. To gain further understanding of the nature of the phase transition, we have carried out measurements of the transition point with improved accuracy for different single-crystal samples. We have found that the samples investigated are classified into two distinct types with respect to the behavior at the phase transition. We have also found that the two types of samples exhibit a marked difference in the high-field Hall effect. In this paper, we focus upon the distinctive behavior of two types of samples and discuss it in terms of possible effect of impurities on the phase transition.

Two things should be remembered in considering this class of materials. First, it is predicted from the Landau-level calculation that an extremely strong magnetic field will eventually lift the band overlap and cause a semimetal-to-semiconductor transition.^{14,15} This phase transition has been observed in $\text{Bi}_{1-x}\text{Sb}_x$ (Ref. 15) at $B = 100$ and 400 kG for $x = 0.065$ and 0.049 , respectively, and more recently in Bi (Ref. 16) at $B = 800$ kG. In the case of graphite, this transition is predicted to occur at $B = 700$ kG,¹⁷ which is outside the experimental range of this work. The semimetal-to-semiconductor phase transition is essentially a one-electron property of the material and should be experimentally distinguishable from those due to many-body effects by the temperature independence of its onset field value.

Another significant consideration is the possibility of ordered states other than the Wigner crystal or the CDW

state. When Landau levels with different spin orientations are populated, the system may undergo a transition into a spin-density-wave (SDW) state.¹⁸ For a semimetallic system, an ordered state called an excitonic phase due to the electron-hole pair condensation is a possible ground state.¹⁹ Bismuth²⁰ and Bi-Sb alloys²¹ have been studied in the context of the excitonic phase transition. But no firm evidence for the phase transition has yet been reported.

II. THEORETICAL MODEL

In this section, the theoretical model of the magnetic-field-induced CDW transition by Fukuyama² and by Yoshioka and Fukuyama¹³ is briefly reviewed. Fukuyama² has considered a situation relevant to a degenerate semiconductor in a very strong magnetic field, where only the lowest spin-split Landau level is left in the vicinity of the Fermi level. In this extreme quantum limit, the energy spectrum of the system becomes identical to that of a one-dimensional system apart from the Landau degeneracy factor $1/2\pi l^2$, where $l = (\hbar c / eB)^{1/2}$ is the Larmor radius. Accordingly, the system has an inherent instability against a perturbation with wave vector $q = 2k_F$, as in the case of a one-dimensional system.²² For an arbitrarily weak attractive electron-electron interaction V at $q = 2k_F$, the system undergoes (in the mean-field approximation) a phase transition to a CDW state at a transition temperature given by

$$k_B T_c = 1.14 \epsilon_F \exp[-1/N(\epsilon_F)V], \quad (1)$$

where $N(\epsilon_F)$ denotes the density of states at the Fermi level.

Now we turn to the case of graphite. Figure 1 shows the Landau-level structure of graphite at $B = 250$ kG applied parallel to the c -axis. The following points should be noted.

(a) In the field range $80 < B < 700$ kG, only the lowest electron Landau level ($n=0$) and the lowest hole Landau level ($n=-1$) are populated.

(b) Both levels are spin split to yield four levels as shown in Fig. 1. Each of the four levels has twofold degeneracy corresponding to the two nonequivalent edges, H - K - H and H' - K' - H' of the Brillouin zone.

(c) In contrast to the case of degenerate semiconductors where the total carrier density is fixed, the carrier density of graphite increases approximately linearly with B , for $100 < B < 500$ kG. The carrier density at helium temperature is $n_e = n_h = 3 \times 10^{18} \text{ cm}^{-3}$ at $B = 0$ and increases to $1.5 \times 10^{19} \text{ cm}^{-3}$ at $B = 250$ kG.

(d) Because of the weak field dependence of the separation between the $n=0$ and the $n=-1$ levels, ϵ_F and k_F are only weakly field dependent for $B < 500$ kG.

Figure 2 illustrates a simplified model for the present system. Note that the Fermi level is located in the flat middle part of the density-of-states curves; hence $N(\epsilon_F) \propto B$ due to the Landau degeneracy factor. This is the case for $100 < B < 500$ kG.

Yoshioka and Fukuyama¹³ have applied Fukuyama's theory to the present case. Since there are four subbands,

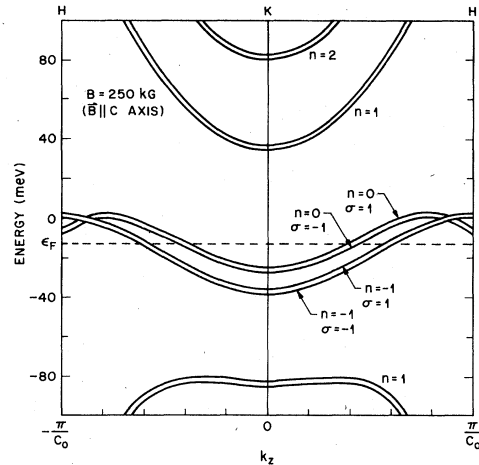
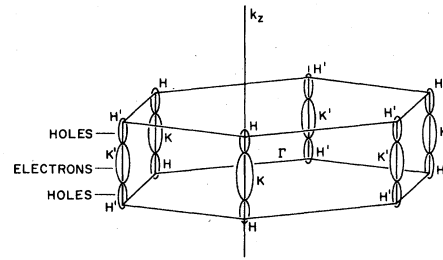


FIG. 1. Landau levels of graphite in a magnetic field of 250 kG along the c axis. The top shows the Brillouin zone and the Fermi surface at $B=0$. Note that there are two nonequivalent edges H - K - H and H' - K' - H' , around which the electron and hole Fermi surfaces are located.

different kinds of instabilities are possible, including CDW, SDW, and excitonic instabilities, corresponding to different nesting wave vectors. Yoshioka and Fukuyama have calculated the transition temperature for each of the instabilities in the Hartree-Fock approximation, and have concluded that the CDW instability associated with the $2k_F$ for the ($n=0, \sigma=1$) subband has the highest T_c . The transition temperature is given by

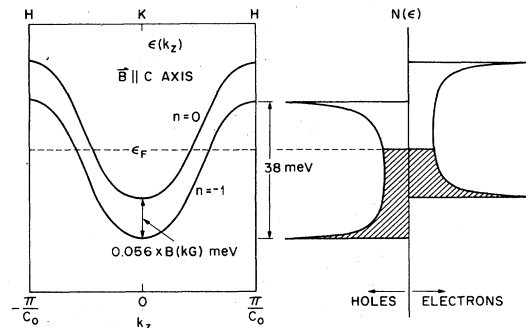


FIG. 2. Schematic subband structure of the present system. The figure on the right-hand side is the density of states. The scale of the density of states is proportional to B , due to the Landau degeneracy.

$$T_c = 4.53 \frac{\epsilon_F}{k_B} \frac{\cos^2(c_0 k_{F0\uparrow}/2)}{\cos(c_0 k_{F0\uparrow})} \times \exp \left\{ - \left[\frac{\tilde{u}}{(2\pi l)^2} \left(\frac{dk_z}{d\epsilon_{0\uparrow}} \right)_{\epsilon_F} \right]^{-1} \right\}, \quad (2)$$

where $c_0 = 6.70 \text{ \AA}$ is the c -axis lattice constant, $\epsilon_{0\uparrow}$ is the energy for the ($n=0, \sigma=\uparrow$) subband, and \tilde{u} is the exchange interaction responsible for the pairing. By choosing the value of the dielectric constant (somewhat arbitrarily) as $\epsilon=10$, they have obtained a good correspondence with the experimental field dependence of T_c . One should be reminded of the sensitivity of T_c calculation to the choice of parameters and of the possible overestimation of T_c using the mean-field theory.

III. EXPERIMENT

The samples used in the present experiment were selected from several batches of Kish graphite which is form of single-crystal graphite prepared by precipitation from a carbon-saturated molten iron or nickel. A natural single-crystal sample was also studied. Table I lists parameters for a representative selection of samples used in the high-field experiment.

The Kish samples were made by Toshiba Ceramics Co., Japan. Unfortunately, detailed records of the crystal-growth conditions and of the purification procedures are not available to us. The known facts about the present samples are as follows.

(1) The batches a and b were produced in one series of furnace operations, whereas the batches c and d were prepared in another series using a different furnace.

(2) The batches a, b, and c have gone through the purification procedure, i.e., heat treatment above 2400°C in a chlorine-gas flow.

(3) The batch d is an as-grown batch.

(4) No information is available for the batches e and f.

The concentration of transition-metal impurities in the

purified samples was found to be below the detectable level of a spectroscopic analysis, i.e., less than a few ppm. The flux material of 10-ppm order of magnitude concentration was detected in the as-grown samples. On the other hand, a magnetic susceptibility measurement indicated the presence of a significant amount of segregated flux material in those samples. Therefore, the concentration of dissolved impurities, which contribute to the carrier scattering, is presumably much lower than the nominal value obtained by the spectroscopic analysis. This inference is supported by the fact that no systematic difference in the transport properties is found between the batch c and the batch d. It seems that the purification procedure is not as effective against the dissolved impurities as it is against the segregated impurities.

The values of residual resistivity ratio (RRR) defined by $R_{300\text{K}}/R_{4.2\text{K}}$ are given in Table I. Little correlation, however, was found between the RRR values for these samples and the behavior exhibited at the phase transition.

The crystals were thin flakes of polygonal shape with the c axis perpendicular to the flake surface. Typical dimensions were 5 mm^2 in area and 0.1 mm in thickness. Crystals of reasonably well-defined shape were selected for the galvanomagnetic measurements. Six electrical leads were attached to each sample using silver paint. Both the magnetoresistivity ρ_{xx} and the Hall resistivity ρ_{xy} were measured by the conventional dc four-probe method with the magnetic field along the c axis (or z axis) and the current in the basal plane. For the Hall-resistivity measurement, an externally attached potentiometer was used to eliminate the misalignment voltage. The largest errors in the absolute values of ρ_{xx} and ρ_{xy} come from the uncertainty in the geometrical factors, and are estimated to be about 30%.

The high-field measurements were carried out using the facilities of The Francis Bitter National Magnet Laboratory at the Massachusetts Institute of Technology. The major part of the experiment was done in a hybrid magnet capable of generating fields up to 290 kG .²³ A conven-

TABLE I. List of graphite samples. a–f: Kish graphite (a–c, purified; d, as-grown). g: natural single crystal (Ticonderoga graphite).

Sample	Batch	$\frac{R_{300\text{K}}}{R_{4.2\text{K}}}$	σ_{xx} σ_{xy}		$n_e - n_h$	T^*	B^*
			[$(\Omega \text{ cm})^{-1}$]				
			$B = 200 \text{ kG}$		(10^{15} cm^{-3})	(K)	(kG)
type A							
1	a	21	8.7	−0.19	2.4	58	1011
2	a	25	9.3	−0.22	2.7	64	1031
3	b	18	11.4	−0.23	2.8	57	1005
4	g	11	19.2	−0.31	3.9	75	1050
type B							
5	c	29	8.0	−1.9	24	92	1142
6	c	23	9.6	−2.8	35	118	1185
7	c	22	8.4	−2.3	28	124	1195
8	d	26	8.3	−1.1	14	134	1220
9	e	17	13.2	−1.3	16	107	1167
10	f	21	6.7	−1.7	21	120	1193

tional Bitter magnet with maximum field of 225 kG was used for preselection of the samples for the hybrid magnet runs. The capability of reversing the field direction in the 225-kG magnet was useful for an accurate measurement of the Hall resistivity. The alignment of the sample position to the center position of the magnet was done accurately by monitoring the sharp Shubnikov-de Haas feature at 73 kG. Possible angular misalignment of the c axis of the samples from the field direction was no more than a few degrees. The field intensity was determined from the calibrated relation between the magnetic field and the generator current. The overall error in the determination of the field intensity was about 0.3%.

Temperatures down to 0.41 K were achieved by a ^3He evaporation cryostat. Appropriate caution was exercised for the precise determination of the temperature, because the environment in a Bitter magnet, with the mechanical as well as the electromagnetic noise, was somewhat hostile to the cryogenics and thermometry. A bundle of thin, insulated copper wires was placed in the sample space to ensure temperature uniformity throughout the ^3He liquid without suffering from eddy-current heating. The temperature uniformity was constantly monitored by three carbon-resistor thermometers placed at the top, middle, and bottom of the sample space. These carbon resistors were selected from a large batch for their almost identical temperature and field characteristics. With the temperature uniformity ensured in this way, the temperature was determined by measuring the ^3He saturated vapor pressure by a capacitance manometer (MKS Baratron) with resolution of 1 mTorr. The estimated error in the thermometry is about 2 mK. The possible local heating of the samples due to the measurement current or the eddy current was checked by repeating the measurements with different dc levels and different field sweep rates. No significant heating effect was observed as long as the dc was kept below 200 μA and the sweep rate below about 0.5 kG/sec.

IV. RESULTS AND DISCUSSION

The galvanomagnetic properties of graphite in the high-field region have been studied by several workers.²⁴⁻²⁷ In the present study, we have focused upon transport behavior in the extreme-quantum-limit region. The samples investigated in the present study have been found to be classified into two distinct types with regard to their high-field magnetotransport behavior. In the following we shall call them types A and B.

Figure 3 shows experimental traces of ρ_{xx} , for two different samples, one representing the type A and the other the type B. The Shubnikov-de Haas (SdH) oscillations composed of two periods, one due to the electron Fermi surface and the other due to the hole Fermi surface, are seen below 80 kG. The two dips seen at $B=66$ and 73 kG correspond to the passing of the spin-split $n=1$ electron Landau levels through the Fermi level. In the field range above this value, the quantum-limit condition depicted in Figs. 1 and 2 is realized.

A sharp increase of ρ_{xx} is seen in Fig. 3 at the onset points indicated by arrows. The onset point shifts toward lower fields as the temperature is decreased. The relation

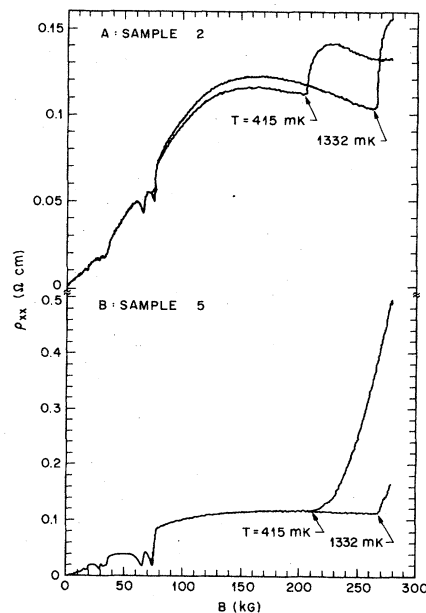


FIG. 3. The transverse magnetoresistivity ρ_{xx} of two samples representative of the two types. Traces at two different temperatures are shown for each sample. Note the marked difference in behavior at the onset of the anomaly for the two sample types.

between the onset point and temperature was determined from traces similar to those shown in Fig. 3. The relation, interpreted as the magnetic field dependence of the transition temperature, is plotted in Fig. 4. The experimental data can be represented by an empirical formula

$$T_c(B) = T^* \exp(-B^*/B), \quad (3)$$

where T^* and B^* are parameters whose values turn out to be about 100 K and 1000 kG, respectively. The values of T^* and B^* for each sample are given in Table I. This empirical formula is to be compared with the BCS formula [Eq. (1)]. As pointed out earlier, $N(\epsilon_F)$ is proportional

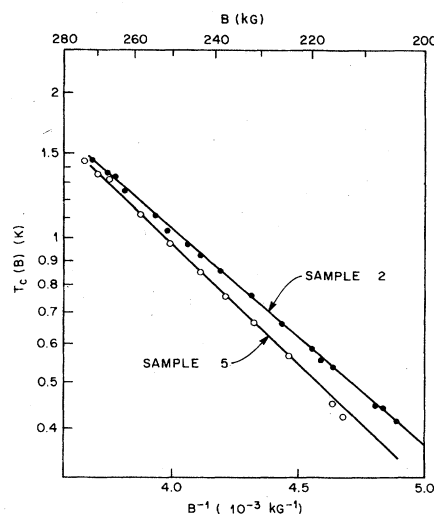


FIG. 4. Magnetic field dependence of the transition temperature.

to B in the present field range. Therefore, if one ignores the possible B dependence of the pairing interaction V in Eq. (1), Eq. (3) can be basically understood as a BCS-type expression for T_c . This BCS-type functional form is consistent with the CDW model by Yoshioka and Fukuyama.¹³ It should be mentioned, however, that since other possible mean-field-type phase transitions should also conform to this functional form, it is premature to draw a conclusion about the precise nature of the new phase.

The experimental results of $T_c(B)$ for different samples taken from the same batch are quite consistent, whereas a systematic difference is found among different batches. As mentioned earlier, the samples can be classified into two types (types A and B), and T_c of the type-B samples is lower than that of the type-A samples by about 100 mK as seen in Fig. 4. Another difference characterizing the two types is the behavior of ρ_{xx} at the transition. Namely, while ρ_{xx} of the type-A samples increases very sharply at the transition, that of the type-B samples shows a less sharp change, as seen in Fig. 3.

In parallel with these differences in the behavior at the transition, we have found an order of magnitude difference in the Hall resistivity between the two types of samples. Figure 5 shows the quantity $-\sigma_{xy}B$ calculated from the ρ_{xx} and ρ_{xy} data, for the same samples as Fig. 3. The high-field Hall conductivity is related to the imbalance between the electron density and the hole density, and is written to first order as

$$\sigma_{xy}B = (n_e - n_h)ec. \quad (4)$$

This quantity should vanish for an ideal pure graphite sample. The vertical axis on the right-hand side of Fig. 5 gives the scale for $n_e - n_h$. The values of $n_e - n_h$ are given in Table I together with the values of σ_{xx} and σ_{xy} at $B=200$ kG. It is seen that the type-B samples have carrier imbalance which is about an order of magnitude larger than the type-A samples. Based on this correlation between the difference in the carrier imbalance and the difference in the behavior at the transition, we discuss the origin of the latter as follows.

First of all, it should be noted that the imbalance itself is only a very small fraction of the total carrier density. Even for the type-B samples, $n_e - n_h$ is less than one percent of n_e ($\approx n_h$) at $B=0$ and is even smaller at high fields. Thus the deviations of n_e and n_h from their ideal values are practically negligible (as evidenced by the absence of any detectable shift of the SdH peak positions), and therefore cannot be the cause of the observed difference in T_c . In fact, a calculation of T_c by use of Eq. (2), with carrier densities differing by such amounts gives at most a T_c difference of ~ 1 mK which is two orders of magnitude smaller than the observed difference.

The imbalance between the electron and the hole density indicates the presence of ionized impurities. The effect of the carrier scattering due to impurities on the phase transition is discussed on the following. The impurity scattering brings about a broadening of Landau levels. The density-of-states curve shown in Fig. 2 is smeared to some extent, and this can in general cause a change in T_c through a change in $N(\epsilon_F)$. For the present case, however, this collision broadening effect cannot cause a signifi-

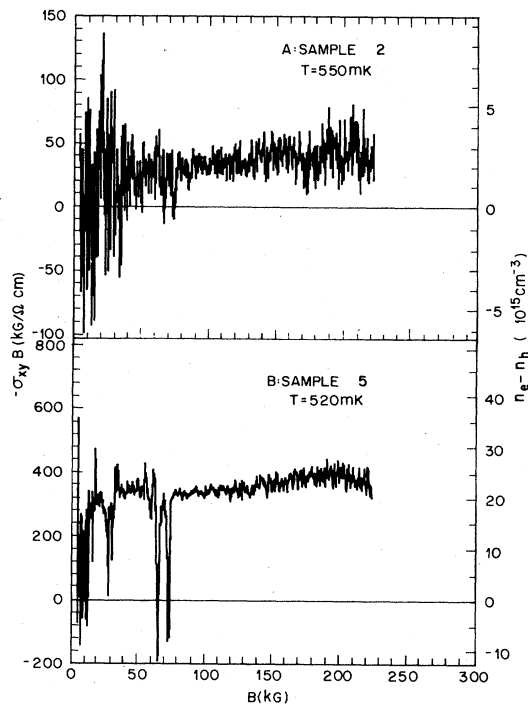


FIG. 5. The quantity $-\sigma_{xy}B$ as a function of B . The scale on the right-hand side gives the difference between the electron and the hole density.

cant change in $N(\epsilon_F)$ because ϵ_F is located in the flat middle part of the density-of-states curve. This is in sharp contrast with the two-dimensional case where the density of states for each Landau level is a delta function in the absence of scattering, so that collision broadening can have a profound effect.

We have seen that the effect of impurities on T_c through the normal-state properties is of minor importance. The effect of impurities on the mean-field-type “pairing” transition has been discussed by several authors.^{28–30} The mathematical formalism of the problem is essentially identical with the case of paramagnetic impurities in a superconductor.³¹ A certain type of impurity scattering has the “pair-breaking” effect and tends to destroy the ordered state. The transition temperature in the presence of impurities is given by

$$\ln \left[\frac{T_c}{T_{c0}} \right] = \psi \left[\frac{1}{2} \right] - \psi \left[\frac{1}{2} + \frac{\hbar}{2\pi k_B T_c \tau} \right], \quad (5)$$

where T_{c0} denotes the transition temperature for a pure material, $\psi(x)$ is digamma function, and τ is the relevant relaxation time due to the scattering processes contributing to the pair breaking. For a large τ , i.e., small impurity concentration, Eq. (5) can be expanded to yield

$$T_c = T_{c0} - \frac{\pi}{4} \frac{\hbar}{k_B} \frac{1}{\tau}. \quad (6)$$

The observed suppression of T_c for the type-B samples by ~ 100 mK compared to the type-A samples can be explained by setting $\tau \sim 6 \times 10^{-11}$ sec in Eq. (6). This value of τ is not inconsistent with the transport relaxation time,

$\tau_{tr} \sim 3 \times 10^{-11}$ sec, estimated from ρ_{xx} using the simple Drude model. (The two relaxation times can be different, as they correspond to different scattering processes.)

We now turn to the behavior of conductivity at the transition. Figure 6 shows σ_{xx} as a function of temperature for different magnetic fields. The transition points are indicated by arrows. We compare the $\sigma_{xx}(T)$ data with the following simple model. We first consider the case without the pair-breaking effect. By the analogy of superconductivity, we may write the temperature dependence of the gap Δ as

$$\Delta(T) = 1.74\Delta(0) \left[1 - \frac{T}{T_c} \right]^{1/2} \quad (T \lesssim T_c), \quad (7)$$

where $\Delta(0)$ is related to T_c by

$$\Delta(0) = 1.76k_B T_c. \quad (8)$$

Considering the possibility that only part of the four subbands participate in the pairing transition, we write σ_{xx} as a sum of the contributions $\sigma_{xx}^{(1)}$ from the subband(s) responsible for the transition and the contributions $\sigma_{xx}^{(2)}$ from the other subbands. We have

$$\sigma_{xx}(T) = \sigma_{xx}^{(1)}(T) + \sigma_{xx}^{(2)}(T). \quad (9)$$

As the gap is opened up at ϵ_F , $\sigma_{xx}^{(1)}(T)$ decreases as $\exp[-\Delta(T)/k_B T]$. If we assume that $\sigma_{xx}^{(2)}(T)$ remains unchanged, the qualitative behavior of $\sigma_{xx}(T)$ is expected to be as the solid curve in Fig. 7. Namely, σ_{xx} decreases sharply at T_c and reaches a limiting value at lower temperatures. Note that the temperature dependence of the

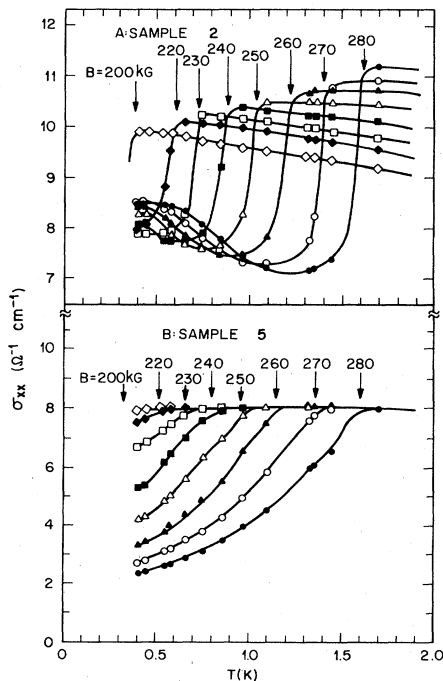


FIG. 6. The conductivity σ_{xx} as a function of temperature for different magnetic fields. The arrows indicate the position of T_c for each magnetic field. The ordered phase occurs below T_c .

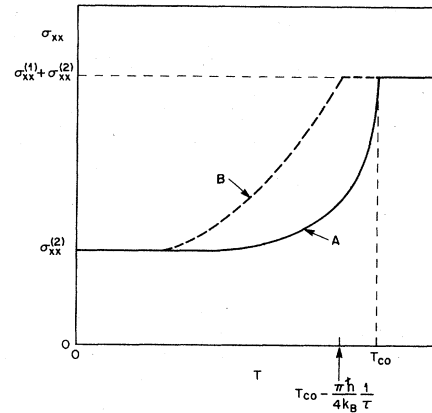


FIG. 7. Schematic temperature dependence of the conductivity according to the simple model described in the text. Curve *A* corresponds to the case of a pure material. Curve *B* represents the case in which "pair breakers" are present. The contributions from the subband(s) responsible for the phase transition are denoted by $\sigma_{xx}^{(1)}$. The contributions from other subbands are denoted by $\sigma_{xx}^{(2)}$.

gap is important only in the narrow region below T_c .

In the presence of pair-breaking impurities, T_c is suppressed according to Eq. (6). Below T_c , the order parameter assumes a finite value, but the gap in the excitation spectrum is not well-defined until the temperature is sufficiently lowered. Because of the presence of this so-called gapless region in the vicinity of T_c , the conductivity change at T_c has a finite slope. The qualitative behavior of $\sigma_{xx}(T)$ for this case is illustrated by the dashed curve in Fig. 7. Comparing Fig. 7 with Fig. 6, we note that the solid and the dashed curves reproduce the qualitative features of the conductivity behavior of the type-A and the type-B samples, respectively.

We have seen that the behavior of the type-B samples with regard to the phase transition is very reminiscent of the manifestation of the pair-breaking effect on the mean-field-type pairing transition. This fact provides additional experimental support for the identification of the observed magnetotransport anomaly with a mean-field-type phase transition. In order to elucidate the impurity effect, it would be best to be able to identify the specific impurities responsible for the effect. Unfortunately, the spectroscopic analysis cannot quantify this level of impurities, and can only set an upper limit of about $5 \times 10^{16} \text{ cm}^{-3}$. At the moment, the only information available for the impurity concentration is that from the transport data.

We have made estimates of the ionized impurity concentrations using the values of carrier imbalance obtained from the high-field Hall-conductivity data. The actual ionized impurity concentrations may differ considerably from such estimates, due to the possible compensation. However, the qualitative trend that the type-B samples contain more ionized impurities than the type-A samples, is unlikely to be upset. Because, in order to be otherwise, the following very unlikely situation has to be assumed. Namely, all the type-A samples must be compensated to a degree better than at least 90%. Moreover, to explain the

observed consistency of the values of $n_e - n_h$, the concentrations of ionized donors and acceptors must be equal for all the type-A samples within a few percent, as contrasted to the observed factor-of-two fluctuation among the type-B samples.

We also point out that there is a qualitative difference between the two sample types in the transport behavior not only in the ordered state ($T < T_c$) but also in the normal state ($T > T_c$). For example, ρ_{xx} for the type-A samples in the quantum limit decreases with decreasing temperature even below 1 K, while that of the type-B samples is temperature independent. Although the mechanism for the temperature dependence at such low temperatures is unknown, this fact suggests that the main scattering processes are different for the two types of samples.

While the ionized-impurity concentrations as deduced from the Hall effect are consistent within each batch of samples, the RRR values show considerable sample dependence. This implies that there is a substantial contribution of neutral scattering centers (neutral impurities or defects). Nevertheless, the transition temperature as a function of field is found to be universal for each batch of samples. This may suggest that the neutral scattering centers are not very effective for the pair-breaking process. On the other hand, the conductivity drop from its normal-state value differs substantially even among samples with same T_c . Generally speaking, the conductivity

change is larger for samples with larger SdH oscillation amplitude. This may be attributed to the difference in the neutral scattering centers.

To summarize, we have made precise measurements of T_c as a function of B on many samples, and have found that $T_c(B)$ is well fitted by the empirical formula, Eq. (3). The samples containing more ionized impurities, as deduced from the Hall effect, show a behavior reminiscent of the pair-breaking effect of the mean-field-type pairing transition. Further study of the impurity effect may provide useful information on the precise nature of the new electronic state of graphite in strong magnetic fields.

ACKNOWLEDGMENTS

We are grateful to L. G. Rubin, B. Brandt, and the staff at the Francis Bitter National Magnet Laboratory for technical assistance. We thank P. M. Tedrow for the loan of the ^3He gas handling system. Helpful conversations with M. S. Dresselhaus, G. Timp, K. Sugihara, H. Fukuyama, D. Yoshioka, P. M. Platzman, H. L. Somner, P. B. Littlewood, H. Suematsu, and S. Tanuma are appreciated. The Kish graphite samples were kindly supplied by H. Suematsu. We acknowledge the Air Force Office of Scientific Research (AFOSR) Contract No. F49620-83-C0011, for support of the MIT part of the work.

¹W. G. Kleppman and R. J. Elliott, *J. Phys. C* **8**, 2729 (1975).

²H. Fukuyama, *Solid State Commun.* **26**, 783 (1978).

³H. Fukuyama, P. M. Platzman, and P. W. Anderson, *Phys. Rev. B* **19**, 5211 (1979).

⁴Y. Kuramoto, *J. Phys. Soc. Jpn.* **44**, 1572 (1978).

⁵R. R. Gerhardt, *Solid State Commun.* **36**, 397 (1980).

⁶D. J. Somerford, *J. Phys. C* **4**, 1570 (1971); C. M. Care and N. H. March, *J. Phys. C* **4**, L372 (1971).

⁷G. Nimtz, B. Schlicht, E. Tyssen, R. Dornhaus, and L. D. Haas, *Solid State Commun.* **32**, 669 (1979); G. Nimtz and B. Schlicht, in *Festkörperprobleme (Advances in Physics)*, edited by J. Treusch (Viewig, Braunschweig, 1980), Vol. XX, p. 369. See also G. De Vos and F. Herlach, in *Application of High Magnetic Field in Semiconductor Physics*, edited by G. Landwehr (Springer, New York, 1983), p. 378.

⁸B. A. Wilson, S. J. Allen, and D. C. Tsui, *Phys. Rev. Lett.* **44**, 479 (1980).

⁹S. Kawaji, J. Wakabayashi, M. Namiki, and K. Kuroda, *Surf. Sci.* **73**, 121 (1978).

¹⁰S. Tanuma, Y. Onuki, R. Inada, A. Furukawa, O. Takahashi, and Y. Iye, in *Physics in High Magnetic Fields*, edited by S. Chikazumi and N. Miura (Springer, New York, 1981), p. 316.

¹¹Y. Iye, P. M. Tedrow, G. Timp, M. Shayegan, M. S. Dresselhaus, G. Dresselhaus, A. Furukawa, and S. Tanuma, *Phys. Rev. B* **25**, 5478 (1982).

¹²G. Timp, P. D. Dresselhaus, T. C. Chieu, G. Dresselhaus, and Y. Iye, *Phys. Rev. B* **28**, 7393 (1983).

¹³D. Yoshioka and H. Fukuyama, *J. Phys. Soc. Jpn.* **50**, 725 (1981).

¹⁴M. Ya Azbel and N. B. Brandt, *Zh. Eksp. Teor. Fiz.* **48**, 1902 (1965) [*Sov. Phys.—JETP* **21**, 804 (1965)].

¹⁵N. B. Brandt and E. A. Svistova, *Usp. Fiz. Nauk* **101**, 249

(1970) [*Sov. Phys.—Uspekhi* **13**, 370 (1970)].

¹⁶N. Miura, G. Kido, and S. Chikazumi, in *Application of High Magnetic Fields in Semiconductor Physics*, edited by G. Landwehr (Springer, New York, 1983), p. 505.

¹⁷K. Nakao, *J. Phys. Soc. Jpn.* **40**, 761 (1976).

¹⁸V. Celli and N. D. Mermin, *Phys. Rev.* **140**, A839 (1965).

¹⁹E. W. Fenton, *Phys. Rev.* **179**, 816 (1968).

²⁰S. Mase and T. Sakai, *J. Phys. Soc. Jpn.* **31**, 730 (1971).

²¹N. B. Brandt and S. M. Chudinov, *J. Low Temp. Phys.* **8**, 339 (1972).

²²See for example, *Low Dimensional Cooperative Phenomena*, edited by H. J. Keller (Plenum, New York, 1975), and *Highly Conducting One-Dimensional Solids*, edited by J. T. Devreese, R. P. Evrard, and V. E. von Doren (Plenum, New York, 1979).

²³M. J. Loupold, J. R. Hale, Y. Iwasa, L. G. Rubin, and R. J. Weggel, *IEEE Trans. Mag.* **MAG-17**, 1779 (1981).

²⁴J. W. McClure and W. J. Spry, *Phys. Rev.* **165**, 809 (1968).

²⁵J. A. Woollam, D. J. Sellmyer, R. O. Dillon and I. L. Spain, in *Low Temperature Physics* (Plenum, New York, 1975), Vol. 4, p. 358.

²⁶N. B. Brandt, G. A. Kapustin, V. G. Karavaev, A. S. Kotosonov and E. A. Svistova, *Zh. Eksp. Teor. Fiz.* **67**, 1136 (1974) [*Sov. Phys.—JETP* **40**, 564 (1975)].

²⁷K. Sugihara and J. A. Woollam, *J. Phys. Soc. Jpn.* **45**, 1891 (1978).

²⁸J. Zittartz, *Phys. Rev.* **164**, 575 (1967); **165**, 605 (1968).

²⁹E. W. Fenton, *J. Low Temp. Phys.* **15**, 637 (1974).

³⁰G. Gomes-Santos and F. Ynduráin, *Phys. Rev. B* **29**, 4459 (1984).

³¹K. Maki, in *Superconductivity*, edited by R. D. Parks (Dekker, New York, 1969), Chap. 18.